

## Isolation of Bioactive Phytochemicals from *Croton macrostachyus* Roots and Their Antibacterial and Molecular Docking Evaluation

Ravi Kumar<sup>1\*</sup>, Neha Sharma<sup>1</sup>, Pankaj Verma<sup>2</sup>

<sup>1</sup>Department of Pharmacognosy, Faculty of Pharmaceutical Sciences, Panjab University, Chandigarh, India.

<sup>2</sup>Department of Biotechnology, Faculty of Life Sciences, Punjabi University, Patiala, India.

\*E-mail ✉ [ravi.kumar@gmail.com](mailto:ravi.kumar@gmail.com)

Received: 28 February 2025; Revised: 08 May 2025; Accepted: 11 May 2025

### ABSTRACT

Medicinal plants remain an important source of antimicrobial agents, particularly in regions where traditional remedies are widely practiced. *Croton macrostachyus* Hochst ex. Delile (Euphorbiaceae) is commonly used in Ethiopian traditional medicine to manage infectious conditions; however, its bioactive constituents and antibacterial mechanisms are not fully understood. This study aimed to identify major phytochemical constituents from the roots of *C. macrostachyus* and to evaluate their antibacterial efficacy using experimental and computational approaches. Root extracts were subjected to silica gel column chromatography, resulting in the isolation of four previously reported compounds. The antibacterial activity of both the crude extracts and purified compounds was tested in vitro against four reference bacterial strains of human pathogens. In addition, molecular docking simulations were carried out to predict the binding interactions of the isolated compounds with *Escherichia coli* DNA gyrase B (PDB ID: 6F86) and *Staphylococcus aureus* Sortase A (PDB ID: 1T2P). Chemical investigation of the root material yielded lupeol,  $\beta$ -sitosterol, stigmasterol, and linoleic acid. Antibacterial assays showed that the extracts and isolated compounds inhibited the growth of the tested pathogens to varying extents. Docking analysis demonstrated stable binding of the compounds within the active sites of both target proteins, with calculated binding energies between  $-7.38$  and  $-5.57$  kcal/mol for DNA gyrase B and  $-7.40$  and  $-5.54$  kcal/mol for Sortase A. The combined experimental and in silico findings suggest that *C. macrostachyus* roots contain bioactive metabolites with antibacterial potential. These results provide mechanistic support for the traditional application of this plant in Ethiopia for the management of infectious diseases, including skin and respiratory ailments.

**Keywords:** Phytochemicals, *Croton macrostachyus*, Antibacterial activity, Molecular docking

**How to Cite This Article:** Kumar R, Sharma N, Verma P. Cytotoxic Isolation of Bioactive Phytochemicals from *Croton macrostachyus* Roots and Their Antibacterial and Molecular Docking Evaluation. Spec J Pharmacogn Phytochem Biotechnol. 2025;5:273-82. <https://doi.org/10.51847/FcqO7oKUeA>

### Introduction

Antimicrobial resistance has become a major driver of persistent and re-emerging infectious diseases worldwide, placing an increasing burden on healthcare systems and national economies [1]. The declining effectiveness of conventional antibiotics has intensified interest in alternative therapeutic sources, particularly plant-derived compounds that may offer new mechanisms of action against resistant microorganisms [2, 3].

*Croton macrostachyus* Hochst ex. Delile, a member of the Euphorbiaceae family, is a resilient deciduous tree that commonly colonizes disturbed and low-fertility environments such as degraded landscapes, forest margins, slopes, and fallow lands [4, 5]. The species is widely distributed across eastern and western Africa, with natural populations reported in Ethiopia, Eritrea, Kenya, Tanzania, Uganda, and Nigeria.

In Ethiopian ethnomedicine, *C. macrostachyus* is frequently employed to manage diverse health conditions, including parasitic infections, sexually transmitted diseases, dermatological disorders, gastrointestinal complaints, respiratory ailments, neurological conditions, and inflammatory diseases [6]. The plant is known locally by

different vernacular names: “Bakkaniisa” in Afaan Oromoo, “Bisana” in Amharic, and “Annika” in the Wolaita language.

Although the therapeutic use of *C. macrostachyus* is well documented in traditional practice, systematic scientific investigations addressing its chemical composition and antimicrobial potential remain scarce. Therefore, the present work was undertaken to isolate and characterize phytochemical constituents from the roots of *C. macrostachyus*, assess their antibacterial activity under laboratory conditions, and explore their interactions with key bacterial proteins through molecular docking studies.

## Materials and Methods

### *Ethical approval*

This research was conducted following ethical approval granted by the Ethics Committee of Wolaita Sodo University (Approval No. RCS/CNS-67/21).

### *Instrumentation and analytical techniques*

Nuclear magnetic resonance spectra ( $^1\text{H}$  and  $^{13}\text{C}$  NMR) were acquired using a Bruker spectrometer (Darmstadt, Germany), employing deuterated chloroform ( $\text{CDCl}_3$ ) as the solvent and tetramethylsilane (TMS) as the internal standard. Melting point measurements were performed using a Mettler Toledo FP62 apparatus. Thin-layer chromatography was carried out on silica gel 60 F<sub>254</sub> plates (Merck, Germany) to monitor fraction purity. Column chromatography was conducted using silica gel (60–120 mesh) for compound separation. Bacterial growth inhibition was evaluated by measuring absorbance at 595 nm with a CLX800 ELISA microplate reader (Bio-Rad, France).

### *Chemicals and microbiological media*

Analytical-grade solvents, including dichloromethane, ethyl acetate, methanol, and chloroform, were used throughout the study. Reagents such as mercuric chloride, potassium iodide, ferric chloride, sulfuric acid, and ammonia were obtained at analytical purity. Mueller–Hinton agar (MHA) (Oxoid, UK) served as the culture medium for antibacterial assays, while dimethyl sulfoxide (DMSO) (Sigma, USA) was employed as a solvent control.

### *Collection and processing of plant material*

Root samples of *C. macrostachyus* were harvested from the Wolaita region of Ethiopia in October 2021. Following collection, the plant material was cleaned thoroughly with running water to remove adhering contaminants and dried under shade at room temperature. Botanical authentication was performed at the Herbarium of the Department of Biology, Addis Ababa University, Ethiopia, and a voucher specimen was deposited under the reference number CM-002/21. The dried roots were subsequently chopped into smaller pieces and pulverized into a fine powder using an electric milling device.

### *Extraction and isolation of compounds*

Air-dried roots of *Croton macrostachyus* were pulverized, and 400 g of the resulting powder was subjected to solvent extraction. The material was first soaked in dichloromethane (1.5 L) and agitated continuously for 24 h at room temperature using a mechanical shaker. After extraction, the mixture was filtered under reduced pressure, and solvent removal was performed using a rotary evaporator at 40 °C to obtain the dichloromethane crude extract. The plant residue was then exhaustively extracted with methanol (1.5 L) following the same procedure to produce the methanolic extract.

For compound isolation, 22 g of the dichloromethane extract was loaded onto a silica gel column and fractionated using a gradient solvent system. Elution commenced with n-hexane containing 5% ethyl acetate, followed by gradual increases in ethyl acetate concentration, and finally methanol (1–10%) in ethyl acetate. Eluates were collected as 102 fractions of 25 mL each. Early elution with 5% ethyl acetate in n-hexane produced compound (1) as a white amorphous solid (21 mg). A precipitate formed in fraction 15 (15% ethyl acetate in n-hexane), which was isolated by filtration and purified with n-hexane to yield compound (4) as white needle-like crystals (18 mg).

Intermediate fractions (25–32), obtained using 25–30% ethyl acetate in n-hexane, displayed two dominant TLC spots. These fractions were combined and rechromatographed on silica gel using a constant solvent system of 15% ethyl acetate in n-hexane. From the resulting 26 subfractions, compound (2) (16 mg) and compound (3) (18 mg) were obtained from subfractions 10 and 14, respectively.

#### *Bacterial strains*

Antibacterial testing was conducted using four standard bacterial strains: two Gram-positive species, *Staphylococcus aureus* (CECT 59) and *Bacillus cereus* (ATCC 700603), and two Gram-negative species, *Escherichia coli* (CECT 434) and *Salmonella Typhi* (ATCC 25931). The strains were sourced from Ethiopian public health institutions (<http://www.eph.gov.et/>) and maintained at  $-4\text{ }^{\circ}\text{C}$  until experimentation at the Microbiology Laboratory of Wolaita Sodo University.

#### *Evaluation of antibacterial activity*

The antibacterial potential of *C. macrostachyus* extracts and purified compounds (1–4) was assessed using the agar disc diffusion assay following the protocol of Balouiri *et al.* [7], with slight procedural adjustments. Test bacteria were cultured on nutrient agar and incubated at  $37\text{ }^{\circ}\text{C}$  prior to use. Stock solutions of each extract and isolated compound were prepared in DMSO (100  $\mu\text{g}/\text{mL}$ ), and working solutions were obtained at concentrations of 25, 50, and 100  $\mu\text{g}/\text{mL}$ .

Bacterial suspensions were standardized to approximately  $10^8$  CFU/mL using the McFarland turbidity standard and uniformly spread onto Mueller–Hinton agar plates. Sterile paper discs (6 mm diameter) impregnated with test solutions were placed onto the inoculated media. Following incubation at  $37\text{ }^{\circ}\text{C}$  for 24 h, antibacterial activity was quantified by measuring inhibition zone diameters. All assays were carried out in triplicate. DMSO (10%) served as the negative control, whereas ciprofloxacin was included as the positive reference drug.

#### *Minimum inhibitory concentration assay*

Minimum inhibitory concentrations were determined using a broth microdilution method in 96-well plates. Serial two-fold dilutions of test samples were prepared in nutrient broth to achieve concentrations between 100 and 1.56  $\mu\text{g}/\text{mL}$ . The assay was performed according to the method described by Balouiri *et al.* [7]. Each well received 10  $\mu\text{L}$  of bacterial inoculum to achieve a final density of approximately  $10^5$  CFU/mL. Growth controls, negative controls (medium only), and positive controls (ciprofloxacin) were included. Plates were incubated at  $37\text{ }^{\circ}\text{C}$  for 24 h, and bacterial growth was assessed by measuring absorbance at 595 nm. MIC values were reported in  $\mu\text{g}/\text{mL}$ .

#### *Molecular docking study*

In silico docking studies were conducted using the Molecular Operating Environment (MOE) software to predict interactions between isolated compounds (1–4) and two bacterial enzymes: DNA gyrase B from *E. coli* (PDB ID: 6F86) and Sortase A from *S. aureus* (PDB ID: 1T2P). Ligand structures were sketched using ChemDraw 16.0, converted to three-dimensional formats, protonated at physiological pH (7.0), and energy minimized using the MMFF94x force field.

Protein crystal structures were retrieved from the Protein Data Bank and processed according to established preparation protocols [8], including removal of bound ligands, cofactors, and selected water molecules. Docking grids were defined to encompass the active binding regions of each enzyme. For each ligand, up to five binding poses were generated, and the conformation with the lowest binding free energy (S-score) was selected for interaction analysis.

## **Results and Discussion**

Solvent extraction of *C. macrostachyus* roots yielded 24.6 g (8.2%) of dichloromethane extract and 30.2 g (10.1%) of methanol extract. Qualitative phytochemical screening revealed the presence of multiple secondary metabolites, including alkaloids, triterpenoids, flavonoids, steroids, tannins, and phenolic compounds. Tannins were not detected in the dichloromethane extract (**Table 1**). These observations are consistent with previously published reports by Tensay G. Kiristos *et al.* [9, 10].

**Table 1.** Qualitative phytochemical screening results of *Croton macrostachyus* root extracts

Phytochemical class	Test reagent(s) used	Dichloromethane extract	Methanol extract
Alkaloids	Mayer's reagent	Present (+)	Present (+)
Steroidal compounds	Chloroform followed by concentrated H <sub>2</sub> SO <sub>4</sub>	Present (+)	Present (+)
Terpenoid compounds	Chloroform and concentrated H <sub>2</sub> SO <sub>4</sub>	Present (+)	Present (+)
Tannins	Ferric chloride (FeCl <sub>3</sub> )	Absent (-)	Present (+)
Flavonoids	Dilute ammonia solution	Present (+)	Present (+)
Phenolic compounds	Ferric chloride (FeCl <sub>3</sub> )	Present (+)	Present (+)

Compound 1 was obtained as a white, non-crystalline solid and exhibited a melting range of 214–217 °C. Analysis of the <sup>1</sup>H NMR spectrum revealed seven methyl resonances (–CH<sub>3</sub>) appearing at δ 1.67, 1.05, 0.97, 0.86, 0.83, 0.82, and 0.79. Signals attributable to a terminal olefinic methylene group (–CH<sub>2</sub>) were observed at δ 4.68 and 4.56 as doublets of doublets (J = 2.5, 1.2 Hz, 2H, H-29a and H-29b). In addition, a downfield resonance at δ 3.18 (dd, J = 10.9, 5.3 Hz, 1H) was assigned to an oxygenated sp<sup>3</sup> methine proton at C-3. The overall proton resonance pattern was indicative of a pentacyclic triterpenoid framework.

The <sup>13</sup>C NMR and DEPT-135 spectra showed a total of 30 carbon resonances. Among these, signals at δ 150.9 and 109.3 were assigned to a quaternary sp<sup>2</sup> carbon (C-20) and a terminal sp<sup>2</sup> methylene carbon (C-29), respectively. A resonance at δ 79.0 corresponded to an oxygenated sp<sup>3</sup> methine carbon at C-3. On the basis of the combined spectroscopic data and comparison with reported values [11, 12], compound 1 was identified as lupeol (**1**, **Figure 1**), which is known to be a major constituent of Ethiopian *C. macrostachyus*.

Compound 2 was isolated in the form of a white solid with a melting point of 136–137 °C. The <sup>1</sup>H NMR spectrum displayed multiple overlapping methylene and methine signals between δ 1.0 and 1.8, consistent with a steroidal skeleton. Two characteristic resonances at δ 3.54 and δ 5.35 were assigned to H-3 and H-6 of the steroid nucleus. Six methyl proton signals observed at δ 0.68, 0.93, 0.83, 0.81, 0.84, and 1.01 further supported the presence of a steroid framework.

The <sup>13</sup>C NMR spectrum showed 29 distinct carbon signals, including an oxymethine carbon at δ 71.8 and two olefinic carbons at δ 138.3 and 121.7. DEPT-135 analysis indicated the presence of six methyl, eleven methylene, nine methine, and three quaternary carbons. These spectroscopic features, together with comparison to previously reported data [13], led to the identification of compound 2 as β-sitosterol (**2**, **Figure 1**).

Compound 3 exhibited spectral characteristics closely related to those of compound 2, with notable differences in the olefinic region. In the <sup>1</sup>H NMR spectrum, additional resonances at δ 5.00 and 5.14 were detected, indicating the presence of both tri-substituted and di-substituted double bonds. This observation was supported by <sup>13</sup>C NMR data, which revealed 29 carbon signals, including three olefinic carbons at δ 138.3, 129.6, and 121.7. Based on these spectroscopic distinctions and comparison with literature data [11, 13], compound 3 was identified as stigmaterol (**3**, **Figure 1**).

Compound 4 was obtained as a pale-yellow oily substance. The <sup>1</sup>H NMR spectrum showed olefinic proton resonances between δ 5.3 and 5.5, while the remaining proton signals appeared upfield below δ 3.0. The <sup>13</sup>C NMR spectrum revealed a carboxylic acid carbonyl carbon at δ 180.2. Four sp<sup>2</sup> methine carbons were observed at δ 130.0, 129.9, 129.8, and 129.7, confirming the presence of unsaturated carbon–carbon bonds.

Additional carbon signals between δ 20.0 and 34.1 were assigned to methylene carbons, with the resonance at δ 34.1 corresponding to the methylene adjacent to the carbonyl group (C-2). The signal at δ 31.0 was attributed to a methylene group located between two olefinic carbons (C-11), while the terminal methyl carbon appeared at δ 14.0. These spectral characteristics were consistent with those reported for linoleic acid [14], leading to the identification of compound 4 as linoleic acid (**4**, **Figure 1**).

The antibacterial potential of *C. macrostachyus* root extracts and the isolated compounds (1–4) was investigated in vitro using the disc diffusion technique. Both Gram-positive and Gram-negative bacterial strains exhibited sensitivity to the tested samples. The dichloromethane extract demonstrated inhibitory effects against Gram-positive bacteria, producing zones of inhibition ranging from 5.9 ± 0.11 to 18.6 ± 0.45 mm against *Bacillus cereus* and from 7.9 ± 0.65 to 22.8 ± 0.30 mm against *Staphylococcus aureus*.

Similarly, the methanolic extract showed notable antibacterial activity, with inhibition zones measuring 8.6 ± 0.57 to 23.5 ± 0.50 mm against *B. cereus* and 5.3 ± 0.58 to 11.8 ± 0.28 mm against *S. aureus*.

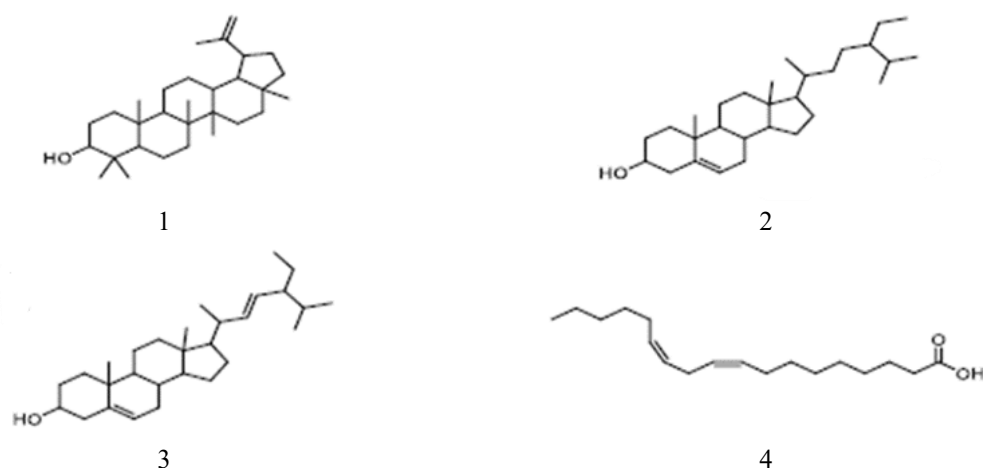


**Figure 1** presents the molecular structures of four secondary metabolites isolated from the roots of *Croton macrostachyus*: lupeol (1),  $\beta$ -sitosterol (2), stigmasterol (3), and linoleic acid (4).

The antibacterial screening revealed that the dichloromethane extract exerted measurable inhibitory effects against Gram-negative bacteria. Inhibition zones of  $6.9 \pm 0.11$  to  $10.6 \pm 0.57$  mm were recorded against *Escherichia coli*, while values between  $4.9 \pm 0.45$  and  $9.3 \pm 0.57$  mm were observed against *Salmonella Typhi*. The methanolic extract showed comparatively weaker activity against Gram-negative strains, producing inhibition zones ranging from  $4.3 \pm 0.57$  to  $8.6 \pm 0.52$  mm against *E. coli*. For *S. Typhi*, inhibition was detected only at the highest tested concentration (100  $\mu\text{g/mL}$ ), yielding a zone of  $5.33 \pm 0.57$  mm.

The antibacterial properties of the purified compounds (1–4) were subsequently evaluated, and the results are summarized in **Table 2**. Both solvent extracts and the isolated constituents demonstrated noteworthy antibacterial efficacy at relatively low concentrations. As illustrated in **Figure 2**, the minimum inhibitory concentration (MIC) values of the extracts varied between 3.75 and 25  $\mu\text{g/mL}$ . Remarkably, the methanol extract exhibited activity comparable to that of the reference antibiotic ciprofloxacin against *Bacillus cereus*, with an MIC of 3.12  $\mu\text{g/mL}$ . All isolated compounds exhibited antibacterial activity to varying extents. Among them, linoleic acid (4) showed the most pronounced inhibitory effect against Gram-positive bacteria, particularly *B. cereus* and *Staphylococcus aureus*. However, this compound did not demonstrate detectable activity against Gram-negative bacterial strains. These findings are in agreement with previously reported studies on similar bioactive compounds [13–18].

DNA gyrase is an essential enzyme for bacterial replication and survival, making it a key target in antibacterial drug discovery [19]. In this study, molecular docking simulations were conducted to assess the interaction of compounds 1–4 with *E. coli* DNA gyrase B. The docking analysis revealed favorable binding affinities for all compounds, with calculated binding energies ranging from  $-5.57$  to  $-7.38$  kcal/mol (**Table 3**). Among the tested ligands, compound 4 achieved the highest docking score. Additionally, compounds 3 and 4 formed hydrogen-bond interactions with critical amino acid residues Arg-76 and Ile-94, respectively. A detailed summary of docking scores, hydrogen bonds, hydrophobic interactions,  $\pi$ -cation contacts, and van der Waals forces is provided in **Table 3** and illustrated in **Figure 3**.

The interaction potential of compounds 1–4 was further examined against *Staphylococcus aureus* Sortase A (PDB ID: 1T2P). Docking results indicated binding energies between  $-5.54$  and  $-7.40$  kcal/mol (**Table 4**), suggesting strong ligand–protein interactions. When compared with the standard antibiotic ciprofloxacin, the isolated compounds showed comparable binding behavior. Notably, compound 4 exhibited a docking score approaching that of ciprofloxacin ( $-7.81$  kcal/mol). Comprehensive interaction profiles, including hydrogen bonding, hydrophobic interactions,  $\pi$ -cation interactions, and van der Waals forces, are summarized in **Table 4** and visualized in **Figure 4**.

**Table 2** summarizes the antibacterial activity of *Croton macrostachyus* root extracts.

Sample	Concentration ( $\mu\text{g/mL}$ )	<i>Bacillus cereus</i>	<i>Staphylococcus aureus</i>	<i>Escherichia coli</i>	<i>Salmonella typhi</i>
DCM extract	100	$18.6 \pm 0.45$	$22.8 \pm 0.30$	$10.6 \pm 0.57$	$9.3 \pm 0.57$
	50	$16.9 \pm 0.36$	$14.36 \pm 0.32$	$6.9 \pm 0.11$	$4.9 \pm 0.45$

	25	5.9 ± 0.11	7.9 ± 0.65	ND	ND
<b>Methanol extract</b>	100	23.5 ± 0.50	11.8 ± 0.28	8.6 ± 0.52	5.3 ± 0.57
	50	17.4 ± 0.40	8.6 ± 0.58	4.3 ± 0.57	ND
	25	8.6 ± 0.57	5.3 ± 0.58	ND	ND
<b>Lupeol</b>	100	12.2 ± 0.37	9.2 ± 0.26	9.7 ± 0.60	7.5 ± 0.50
	50	10.2 ± 0.25	6.3 ± 0.26	6.0 ± 1.00	3.0 ± 1.00
	25	5.5 ± 0.50	3.3 ± 0.57	ND	ND
<b>β-Sitosterol</b>	100	14.1 ± 0.28	12.5 ± 0.50	8.0 ± 0.00	9.0 ± 0.00
	50	10.3 ± 0.57	10.4 ± 0.52	6.0 ± 0.00	7.0 ± 0.00
	25	5.7 ± 0.68	6.0 ± 0.01	3.0 ± 0.00	4.0 ± 0.00
<b>Stigmasterol</b>	100	18.1 ± 0.28	21.3 ± 0.28	11.9 ± 0.11	7.9 ± 0.11
	50	17.0 ± 0.50	17.0 ± 0.00	7.1 ± 0.28	5.1 ± 0.23
	25	11.2 ± 0.14	8.1 ± 0.21	ND	ND
<b>Linoleic acid</b>	100	20.2 ± 0.34	21.0 ± 0.11	ND	ND
	50	16.0 ± 0.11	12.9 ± 0.01	ND	ND
	25	13.23 ± 0.40	8.9 ± 0.00	ND	ND
<b>Ciprofloxacin</b>	5	26	24	28	27

ND: not detected; DCM: dichloromethane

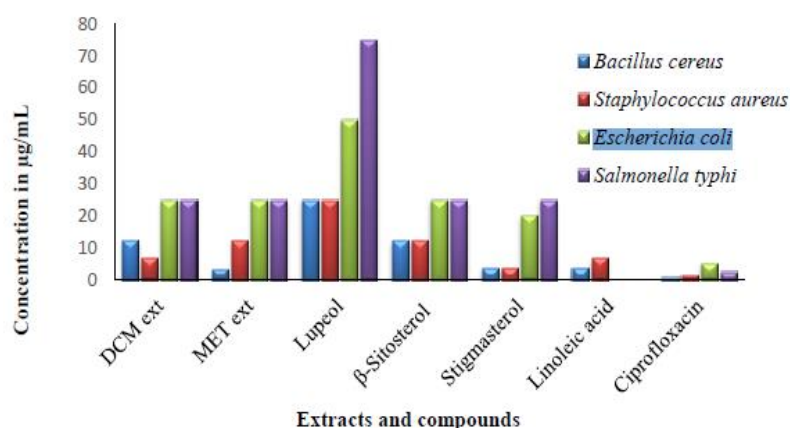
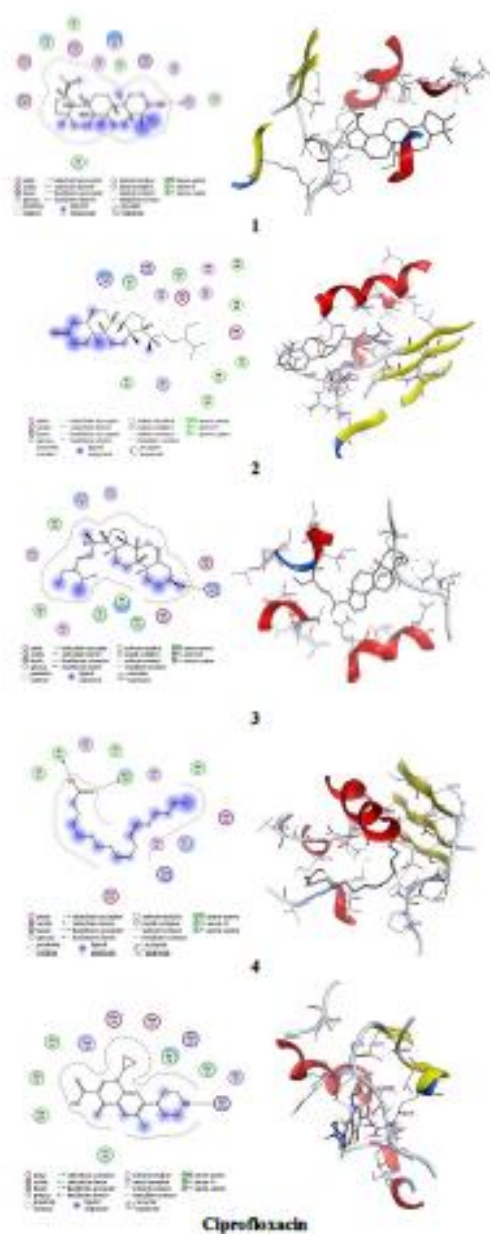


**Figure 2.** Comparative minimum inhibitory concentrations of *Croton macrostachyus* root-derived extracts and purified compounds against the tested bacteria.

**Table 3.** Docking affinity values and key interacting amino acid residues for the isolated phytochemicals targeting *Escherichia coli* DNA gyrase B.

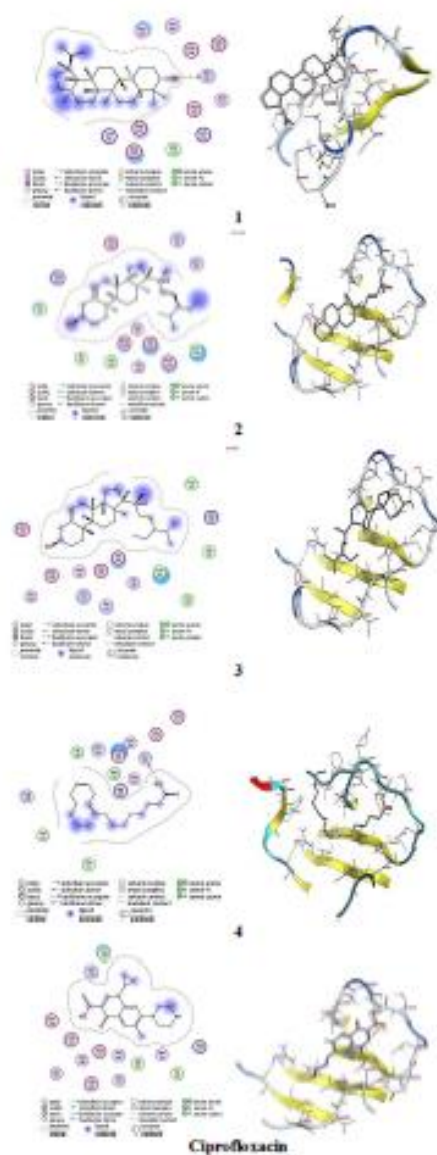
Compound	Binding affinity (S-score, kcal/mol)	Hydrogen bond interactions	Side-chain interactions (donors)	Side-chain interactions (acceptors)	Backbone interactions (donors)	Backbone interactions (acceptors)
<b>Lupeol</b>	-5.57	-	Asp73, Asp49, Glu50	Asn46, Gly77, Gly117, Gly119	Ile78, Pro79, Ile94, Ala47, Val118	Arg76
<b>β-Sitosterol</b>	-5.74	-	Glu50, Asp73	Arg76, Gly77, Arg136, Thr165, Gln72, Asn46	Ile78, Pro79, Met166, Ala47, Ile94, Val43, Val120, Val167	Arg76, Arg138
<b>Stigmasterol</b>	-5.90	Arg76	Glu50, Asp49	Asn46, Gly117, Gly119	Val97, Val118, Leu98, Ile94, Pro79	Arg76
<b>Linoleic acid</b>	-7.38	Ile94	Asp73, Glu50	Asn46, Gly77, Gly119	Ile94, Ile78, Pro79, Ala47, Val43, Val71	Arg76

				Ser121, Thr165	Val97, Val118, Val120, Val167
<b>Ciprofloxacin</b>	-7.42	Arg76, Ile78	Ala47, Pro79	Asn46, Ile78, Glu50, Gly77	Ile78, Pro79, Ala47, Ile94, Val71, Val43, Val97, Val118



### Ciprofloxacin

**Figure 3.** Structural visualization in two and three dimensions illustrating the interaction patterns of lupeol (1),  $\beta$ -sitosterol (2), stigmasterol (3), linoleic acid (4), and the standard antibiotic ciprofloxacin within the binding pocket of DNA gyrase B (PDB ID: 6F86).



#### Ciprofloxacin

**Figure 4.** Two- and three-dimensional depictions of molecular binding interactions between lupeol (1),  $\beta$ -sitosterol (2), stigmasterol (3), linoleic acid (4), and ciprofloxacin with the Sortase A enzyme (PDB ID: 1T2P).

**Table 4.** Predicted docking energies and interacting amino acid residues of the isolated phytochemicals in complex with *Staphylococcus aureus* Sortase A.

Compound	Docking score (kcal/mol)	Hydrogen-bonded residues	Side-chain interaction (donors)	Side-chain interaction (acceptors)	Backbone interaction (donors)	Backbone interaction (acceptors)
$\beta$ -Sitosterol	-6.40	-	Asp112, Asp170, Glu105, Glu108	Asn114, Asn116, Ser109, Thr180	Leu169, Pro163, Val166, Val168	Arg197
Lupeol	-5.54	Ser116	Asp112, Asp170, Glu105, Glu108	Asn107, Asn114, Ser109, Ser116	Leu169	Lys62, Lys173

<b>Linoleic acid</b>	-7.42	Asn107	Glu105, Glu108, Asp112	Gly192, Ser116, Asn114, Ser109	Val193, Pro91, Ile182, Ala104	Arg197
<b>Stigmasterol</b>	-6.98	–	Glu105, Glu108, Asp112, Asp170	Ser116, Asn107, Asn114, Thr180	Pro163, Ile199, Val166, Leu169	Arg197
<b>Ciprofloxacin</b>	-7.81	Ser109, Thr188, Asn107, Gln113, Asn114, Ser116	Glu105, Glu108, Asp112, Asp170	–	Leu169, Ala104, Ile182	Arg197

The advancement of Ethiopian herbal-based therapeutics requires rigorous scientific validation of traditionally employed medicinal plants using internationally accepted methodologies. Despite the exceptional botanical diversity found in Ethiopia, comprehensive chemical profiling and biological assessment of many indigenous medicinal species remain largely unexplored. In this study, four known bioactive constituents—lupeol (1),  $\beta$ -sitosterol (2), stigmasterol (3), and linoleic acid (4)—were isolated and identified from the root material of *C. macrostachyus*. Both the crude root extracts and the purified compounds demonstrated measurable antibacterial effects in laboratory assays.

A comparative evaluation revealed that the crude extracts, obtained using dichloromethane and methanol, produced greater antibacterial inhibition than the individual isolated compounds. This enhanced efficacy is likely a consequence of cooperative or additive interactions among multiple secondary metabolites within the extracts. Notably, the methanolic extract showed broader and stronger inhibitory activity against both Gram-positive and Gram-negative bacterial species than the dichloromethane extract. Among the purified constituents, linoleic acid (4) exhibited the most pronounced antibacterial activity against Gram-positive organisms, achieving inhibitory concentrations comparable to those of the reference drug ciprofloxacin.

Computational docking analyses supported the experimental findings, indicating stable and energetically favorable interactions between the isolated compounds and two key bacterial enzymes, namely *E. coli* DNA gyrase B and *S. aureus* Sortase A. The observed antibacterial properties of the extracts are plausibly linked to their high content of biologically active secondary metabolites, particularly flavonoids, tannins, and alkaloids.

## Conclusion

The findings of this investigation substantiate the ethnomedicinal application of *Croton macrostachyus* in Ethiopia for the treatment of skin-related infections, respiratory ailments, gastrointestinal discomfort, and influenza-like conditions, thereby reinforcing its value within African traditional healthcare systems.

**Acknowledgments:** None

**Conflict of Interest:** None

**Financial Support:** None

**Ethics Statement:** None

## References

1. Spornovasilis N, Tsiodras S, Poulakou G. Emerging and re-emerging infectious diseases: humankind's companions and competitors. *Microorganisms*. 2022;10(1):1–5.
2. Khan R, Islam B, Akram M, Shakil S, Ahmad A, Ali SM, et al. Antimicrobial activity of five herbal extracts against multidrug-resistant strains. *Molecules*. 2009;14(2):586–97.
3. Sibanda T, Okoh AI. Challenges of overcoming antibiotic resistance: plant extracts as potential sources. *Afr J Biotechnol*. 2007;6(25):2886–96.
4. Wakjira K, Negash L. Germination responses of *Croton macrostachyus* to physico-chemical pretreatments.

- S Afr J Bot. 2013;87(1):76–83.
5. Maroyi A. Pharmacological properties of *Croton macrostachyus*: a comprehensive review. *Evid Based Complement Alternat Med*. 2017;Article ID 1694671.
  6. Meresa A, Ashebir R, Gemechu W, Teka F, Basha H, Abebe A, et al. Ethnomedicinal uses and antimalarial effect of *Croton macrostachyus*: a review. *J Med Plants Stud*. 2019;7(2):79–88.
  7. Balouiri M, Sadiki M, Ibsouda SK. Methods for in vitro evaluating antimicrobial activity. *J Pharm Anal*. 2016;6(1):71–79.
  8. Saif R, Hassan RM, Rehman T, Zafar MO, Zia S, Qureshi AR. Molecular docking of *Olea europaea* and *Curcuma longa* compounds targeting SARS-nCoV-2 main protease. *ChemRxiv*. 2022. Available from: <https://chemrxiv.org/engage/chemrxiv/article-details/60c755e0337d6c05cde28d21>.
  9. Teshome M, Adane L, Tariku Y. Phytochemical screening and antibacterial activities of *Moringa stenopetala* root bark extracts. *Res J Med Plants*. 2020;15(1):1–6.
  10. Kiristos TG, Teka MZ, Kebede A, Krishna KC. Phytochemical screening and antibacterial activity of *Croton macrostachyus* stem bark extracts. *Drug Invent Today*. 2018;10(1):2727–33.
  11. Jain PS, Bari SB. Isolation of lupeol, stigmasterol and campesterol from *Wrightia tinctoria*. *Asian J Plant Sci*. 2010;9(3):163–67.
  12. Laghari AH, Memon S, Nelofar A, Khan KM. *Alhagi maurorum* as a source of lupeol. *Ind Crops Prod*. 2011;34(1):1141–45.
  13. Feyera Fufa M, Deressa F, Deyou T, Abdisa N. Isolation and antimicrobial evaluation of compounds from *Melia azedarach* and *Albizia schimperiana*. *Med Chem (Los Angeles)*. 2018;8(6):154–65.
  14. Koroma L, Yormah TBR, Kamara LM, Robert GMT. Extraction and characterization of linoleic acid from *Caloncoba echinata* leaves. *Technol Sci Am Sci Res J Eng*. 2018;45(1):185–206.
  15. Yusuf A, Abdullahi M, Aleku G, Ibrahim I, Alebiosu C, Yahaya M, et al. Antimicrobial activity of stigmasterol from *Neocarya macrophylla* stem bark. *J Med Plants Econ Dev*. 2018;2(1):1–5.
  16. Anas A, Ahmed A, Umar S, Jajere UM, Mshelia EH, Natasha O. Inhibitory effect of lupeol from *Diospyros mespiliformis* against microbial pathogens. *Bayero J Pure Appl Sci*. 2017;10(1):293–99.
  17. Nweze C, Ibrahim H, Ndukwe GI. Beta-sitosterol with antimicrobial activity from *Punica granatum* stem bark. *J Appl Sci Environ Manag*. 2019;23(6):1045–49.
  18. Dilika F, Bremner PD, Meyer JJM. Antibacterial activity of linoleic and oleic acids from *Helichrysum pedunculatum*. *Fitoterapia*. 2000;71(4):450–52.
  19. Collin F, Karkare S, Maxwell A. Exploiting bacterial DNA gyrase as a drug target. *Appl Microbiol Biotechnol*. 2011;92(3):479–97.